



Mechanical, dielectric and EMI shielding response of styrene acrylonitrile, styrene acrylonitrile/polyaniline polymer blends, upon incorporation of few layer graphene at low filler loadings

Abdul Saboor^{1,2} · Ahmad Nawaz Khan¹ · Rahim Jan¹ · Saqib Sharif³ · Munawar Khan¹

Received: 23 May 2018 / Accepted: 5 November 2018 / Published online: 10 November 2018
© Springer Nature B.V. 2018

Abstract

The malfunction of electronic devices and many health-related issues may be caused due to electromagnetic interference (EMI) pollution. To overcome this problem a new set of material SAN/PANI/FLG hybrid composite with better EMI shielding properties is prepared using solution casting technique. Conductive polyaniline (PANI) is added (5 wt% and 10 wt%) to otherwise, an insulative polymer styrene acrylonitrile (SAN). Furthermore, few layer graphene (FLG) is added (0.1–1 wt%) to SAN/PANI polymer blends for preparation of SAN/PANI/FLG hybrid composites. The incorporation of PANI in SAN produces a phase separated morphology, whereas graphene appears in sheet like structure. For 0.1 wt% FLG/SAN/PANI-10 composite, total shielding effectiveness (SE_T) is enhanced from 1.1 to 24.3 dB (100 Hz), mainly due to enhanced dielectric characteristics. However, the maximum increase in tensile strength (49.6 MPa) and modulus (1.5 GPa) is observed for 0.5 wt% FLG/SAN/PANI-5.0 hybrid composite. The increase in dielectric properties and shielding efficiency of SAN/PANI/FLG may be credited to the accumulation of space charges or electric dipoles at the insulator conductor-interface.

Keywords Hybrid composites · EMI shielding · Dielectric properties · Mechanical properties · Polymer blends

Introduction

In recent times, the extensive use of high frequency operated electronic devices have increased the electromagnetic

interference (EMI) pollution. Besides its harmful effects to human health, strong EMI is also the primary cause of reducing the performance of various civil and military electronic devices [1–3]. Materials having dielectric, magnetic and metallic characteristics are often used to reduce the effect of EMI [4–10]. A new set of materials known as hybrid organic composites have prominent advantages over metallic or magnetic materials due to their ease of processing, reduced weight and low cost [11, 12]. The general procedure is to physically combine an insulative polymer with a non-insulative polymer and other nano fillers, which would give the best set of required properties. Different type of nano fillers like CNTs, graphene, ferroelectric ceramics, layered silicates etc., are dispersed in polymer matrix to increase the dielectric response of composite material, and use them, for EMI shielding application [13–21].

Polyaniline (PANI) an excellent conductive polymer, has been used for number of electronic applications. It may not be, used as a single system due to its poor mechanical properties. In order to use its conductive nature, one scheme is to blend PANI with another polymer (used as a matrix) and then add a nano filler (graphene, CNT's,

✉ Abdul Saboor
saboora@gmail.com

Ahmad Nawaz Khan
ahmad.nawaz12@gmail.com

Rahim Jan
rahimjan@scme.nust.edu.pk

Saqib Sharif
saqibaan@gmail.com

Munawar Khan
enr.munawarkhan@gmail.com

¹ School of Chemical and Materials Engineering, National University of Sciences and Technology, Sector H-12, Islamabad, Pakistan

² US-Pakistan Center for Advance Studies in Energy, UET Peshawar, Peshawar, Pakistan

³ Gwangju Institute of Science and Technology (GIST), Gwangju, South Korea

etc.) as a third component to improve dielectric, mechanical and EMI shielding properties [22–24]. M.C. Arenas et al. [25] reported that PVA/PANI nanocomposites were prepared by chemical oxidation synthesis to enhance the electrical conductivity up to 0.044 S/cm with 5 wt% PANI in PVA matrix. Similarly, Saboor et al. [26] investigated that dielectric constant and dielectric loss increased around five and eight orders of magnitude by adding 40 wt% of PANI in SAN matrix at 1 KHz. Varij panwar et al. [27] also reported 5 orders of increase in dielectric constant at 0.029 vol% of graphene in SAN matrix. Similarly the AC conductivity increased to $1.7 \times 10^{-3} \text{ Scm}^{-1}$ near percolation point. The SAN/GNS thin films were prepared using solution casting method. Moreover, graphene possesses high surface area and sizable aspect ratio, therefore, its dispersion in polymer matrices can enhance the properties at low percolation threshold. Khoulood jlassi et al. [28] recently studied an increase in ϵ' from 7.3 to 14.3 with the addition of only 0.5 wt% concentration of B-DPA-PANI in epoxy matrix, whereas the maximum tensile strength of 53.16 MPa was observed at 0.1 wt% of B-DPA-PANI. The increase in mechanical and dielectric properties is due to the suitable network formation of clay/PANI nano filler in epoxy matrix. Recently, Shahzad et al. [29] investigated that by incorporating sulfur doped rGO nanoparticles in PS matrix at 7.5 vol% concentration the shielding efficiency of rGO/PS nanocomposites increased from 21.4 dB to 24.5 dB. Liang et al. [30] prepared epoxy/functionalized-graphene nanocomposites and achieved shielding efficiency of 21 dB at 15 wt% loading. From above discussion it is clear that PANI and graphene may be used together to alter the nature of polymer matrix for the required set of properties.

This research work deals with the mechanical, dielectric and EMI shielding properties of SAN/PANI/FLG hybrid composites prepared by solution casting method. Insulating styrene acrylonitrile (SAN) act as a matrix for both conductive polymer polyaniline (PANI) and few layer graphene (FLG). To prepare SAN/PANI/FLG hybrid composites, first PANI is added at two different concentrations to prepare SAN/PANI conductive polymer blends, which slightly improves the dielectric and EMI shielding properties. In order to further enhance the intrinsic conductive properties and also to impart mechanical strength to SAN/PANI polymer blend, FLG is added. By varying the concentration of FLG in SAN/PANI polymer blend, mechanical as well as dielectric and EMI shielding properties are improved, due to an electrically conducting network formation inside insulative matrix. A considerable increase in EMI shielding (based on dielectric behavior) is observed for free standing thin films of SAN/PANI/FLG hybrid composites.

Experimental section

Materials

ERKOL, Turkey provided commercial grade styrene acrylonitrile (SAN), whereas Uni CHEM chemical reagents supplied aniline monomers, which were then purified through distillation. Ammonium peroxydisulfate (APS) (99% pure) was purchased from Daejung chemicals, Korea. Sodium dodecyl sulphate (SDS) was purchased from Sigma Aldrich. Few layer graphene (FLG) having 5–8 layers on average, produced through mechanical thinning process, was provided by I. Janowska [31]. FLG contained carboxylic and hydroxyl groups which helped in better dispersion of FLG in polymer matrix.

Preparation of polyaniline

Chemical oxidation polymerization technique was used to prepare conductive Polyaniline (PANI). To initiate the reaction, in 100 ml of Deionized water 6 g of aniline monomer (ANI) was added in a flask containing a magnetic stirrer, the whole assembly was placed in ice bath in order to maintain the temperature at 0° C. 1 M HCL acid solution was added to make it conductive, which produced aniline hydrochloride after continuous stirring. Sodium dodecyl sulphate (SDS) used as a surfactant, was added at 1 M concentration. To start the polymerization process, an initiator ammonium peroxide sulphate (APS) in concentration of 1.2 g was dissolved in 20 g deionized water. The solution was added slowly to the aniline solution at a constrained temperature of 0° C with 1 h stirring, followed by stirring for 1.5 h at ambient temperature. Methanol was used to precipitate the polymer, then washed several times with distilled water, followed by drying in vacuum oven at 50° C. A green colored powder of PANI was obtained as final product.

Thin films preparation

Polymer blends

Solution casting technique was used to prepare thin films of polymer blends. The weighed amount of SAN was dissolved in 40 min in 1, 2 dichloroethane through continuous stirring. Afterwards, PANI powder, dried in vacuum oven at 60° C to remove any moisture, was added in 5 and 10 wt% concentrations into SAN, termed as SAN/PANI-5 and SAN/PANI-10 respectively. The SAN/PANI solution was first sonicated for 1 h by probe sonicator for better mixing and then stirred for 24 h. The solution was added to petri dishes and then dried over-night (fume hood) in an ambient environment. For further drying SAN/PANI polymer blends were placed in vacuum oven at 60° C for 5 h.

Hybrid composites

For preparing SAN/PANI/FLG hybrid composite, few layer graphene was added to two concentrations of SAN/PANI blends. Solution casting method was used in which required amounts of FLG (0.1, 0.5, and 1 wt%) was dispersed by stirring and sonication in the SAN/PANI solution. First probe sonication was done for 1 h and after sonication the solution was stirred for 24 h. The solution was then casted in petri dishes for over-night drying in a fume hood at room temperature, further drying was done in vacuum oven. Thickness of prepared casted films of hybrid composites were about 0.1 mm.

Characterization techniques

Differential scanning calorimetry (DSC)

Diamond DSC (Perkin Elmer Pyris) provided with liquid N₂, was used to study the thermal behavior of hybrid composites. The DSC furnace was purged by dry N₂ at a flow rate of 10 mL/min. The heating rate of 10° C/min was used, whereas the weight of sample was kept ~ 5 mg. The rate of heat flow and temperature were graded with zinc and indium standards.

Scanning Electron microscopy (SEM)

To explore the morphology of sample Analytical Scanning Electron Microscope (JOEL JSM-6490A) was used. Casted films were cryogenically cracked using liquid Nitrogen to study the cross section of polymer sample. Ion sputtering device (JOEL JFC-1500) was used to coat the polymer samples with thin layer of gold.

Mechanical properties

Trapezium-X Universal Testing Machine AG-20KNXD Plus was used to determine the mechanical behavior. The cross-head speed was 5 mm/min (ASTM D882). Hand cutter was used to cut the specimens according to the dimensions of 80 × 10 × 0.1 mm³ (length x width x thickness) with a gauge length of 20 mm (ASTM D6287). Five samples were tested at ambient temperature to obtain an average value.

Dielectric properties

To determine the Dielectric response, Wayne Kerr 6500B precision impedance analyzer was used at ambient temperature. Circular samples with thickness of 0.1 mm and diameter of 13 mm were cut from casted films. The dissipation D and capacitance C were measured with respect to frequency ranging from 100 Hz to 5 MHz.

Analysis of dielectric data

Dielectric response is represented in terms of real (ϵ') and imaginary part of dielectric permittivity (ϵ'') acquired from the complex permittivity $\epsilon = \epsilon' - i\epsilon''$ [32]. Materials ability to store electrical energy in an electric field is called dielectric constant, which can be calculated by the following equation.

$$\epsilon' = \frac{Cd}{A\epsilon_0} \quad (1)$$

Sample's capacitance is represented by C , thickness by d in meters, area in meters by A , whereas permittivity of free space is represented by ϵ_0 . To calculate dielectric loss, tangent loss ($\tan\delta$) is used measured directly from instrument, which is having the following expression;

$$\tan\delta = \frac{\epsilon''}{\epsilon'} \quad (2)$$

Dissipation factor D ($\tan\delta$), which is a measure of the energy dissipated by the dielectric material under an oscillating field. AC conductivity of hybrid composites is measured using the following formula;

$$\sigma_{AC} = \omega\epsilon_0\epsilon' \tan\delta \quad (3)$$

ϵ' , ϵ'' , $\tan\delta$ and σ_{AC} are obtained at ambient temperature with respect to frequency.

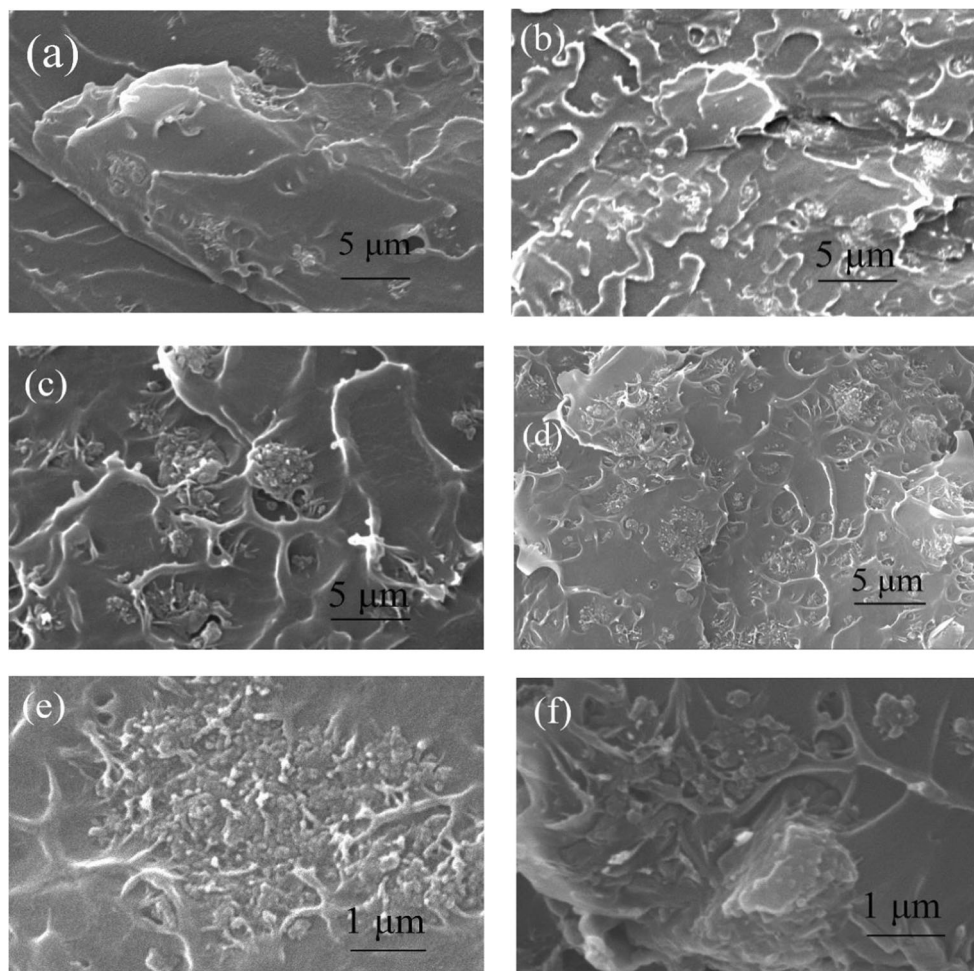
Results and discussion

Structure and morphology

Figure 1 shows the SEM images of SAN/PANI-5&10 polymer blends with 0.5 wt% concentration of FLG. For SAN/PANI polymer blends (Fig. 1a, b) the vivid lines indicates the distribution of PANI. It indicates the heterogeneous morphology owing to the immiscibility of both SAN and PANI phase. The uniform distribution of PANI phase in SAN is evident at high loading (10%) as shown Fig. 1b. Figure 1c, d shows the morphology of both hybrid composites, the sheet like structure of FLG can be seen when the resolution is increased up to 1 micro meter (Fig. 1e, f). A proper interconnected network of both PANI phase and few layer graphene in SAN is formed (Fig. 1d), which indicates nice distribution of PANI and FLG in SAN matrix.

The DSC results of SAN, PANI and SAN/PANI-5&10 polymer blends with varying amount of FLG from 0.1 wt% to 1 wt% are shown in Fig. 2. The glass transition temperature T_g for neat SAN in Fig. 2a, b is clearly indicated by a step

Fig. 1 SEM Photograph of (a) SAN/PANI-5.0%, **b** SAN/PANI-10%, **c** SAN/PANI-5%/FLG-0.5%, **d** SAN/PANI-10%/FLG-0.5. Zoomed SEM images of FLG (0.5 wt%) at 1micrometer (e), (f)



appeared at 105 °C, whereas the T_g for pure PANI is shown at 162.8 °C. The inclusion of PANI in SAN at 10 wt% slightly reduces the T_g of SAN to 103 °C, whereas no considerable change occurs in T_g at 5 wt% loading of PANI as shown in Fig. 2a, b. The addition of PANI at 10 wt% concentration reduces the thermal stability of SAN, as the chain mobility takes place at lower temperatures. The incorporation of FLG at 0.1 wt% in both polymer blends i.e. SAN/PANI-5&10 (5 & 10 wt%), increases the T_g to 109 °C, which indicates that thermal resistance has been increased, [33–35] whereas the step for T_g gets broadened at 0.5 wt% concentration of FLG, which may represent the formation of heterogeneous phase morphology of SAN/PANI/FLG hybrid polymer composites. The results are in consistency with SEM results.

The heterogeneous phase morphology for SAN/PANI/FLG hybrid polymer composites is confirmed by the SEM and DSC results. The combination of both PANI and FLG in SAN matrix are forming interconnected phase, which would probably impact the dielectric and mechanical properties of SAN.

Mechanical properties

The mechanical behavior of hybrid composites is explained by stress strain curves as shown in Figs. 3 and 4. The incorporation of PANI at two different concentration i.e. at 5 wt% and 10 wt% in SAN matrix reduces the mechanical response, however changing concentrations of few layer graphene (FLG) i.e. from 0.1 wt% to 1 wt% in both SAN/PANI polymer blends not only increases the strain at break but also increases the tensile strength and Young's modulus. In SAN/PANI-5.0 hybrid composites (Fig. 3), the addition of PANI at 5 wt% concentration in SAN matrix reduces the strain at break from 4.9% to 3.5%, whereas the tensile strength and young modulus also reduces to 30.9 MPa and 1.2 GPa from 33.14 MPa and 1.38 GPa, respectively. By addition of FLG to SAN/PANI-5.0 blend, mechanical characteristic is enhanced. The strain at break is increased from 4.9% to 6.9% at 0.5 wt% FLG. The tensile strength and Young's modulus are increased from i.e. 33.14 MPa to 49.6 MPa, and 1.38 GPa to 1.5 GPa, respectively at 0.5 wt% concentration of FLG. Further increase in FLG loading to 1 wt% in SAN/PANI-5.0 polymer blend reduces the strain at break, tensile strength and modulus to 4.27%,

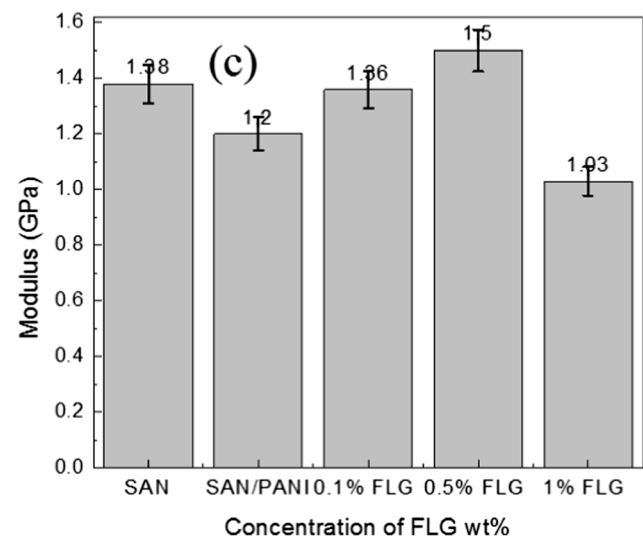
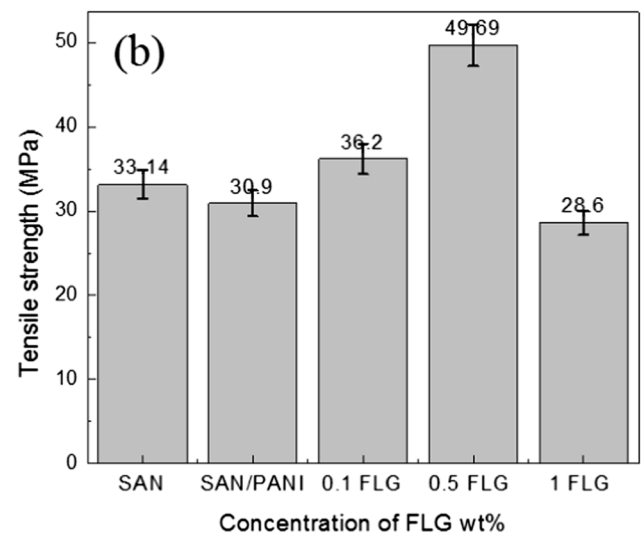
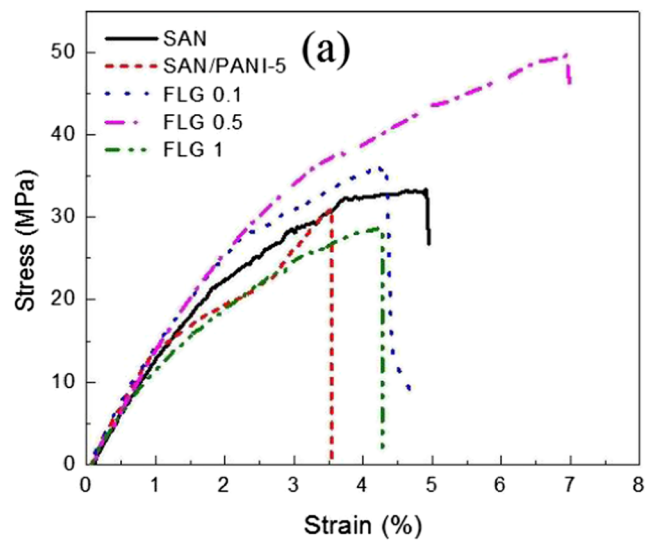
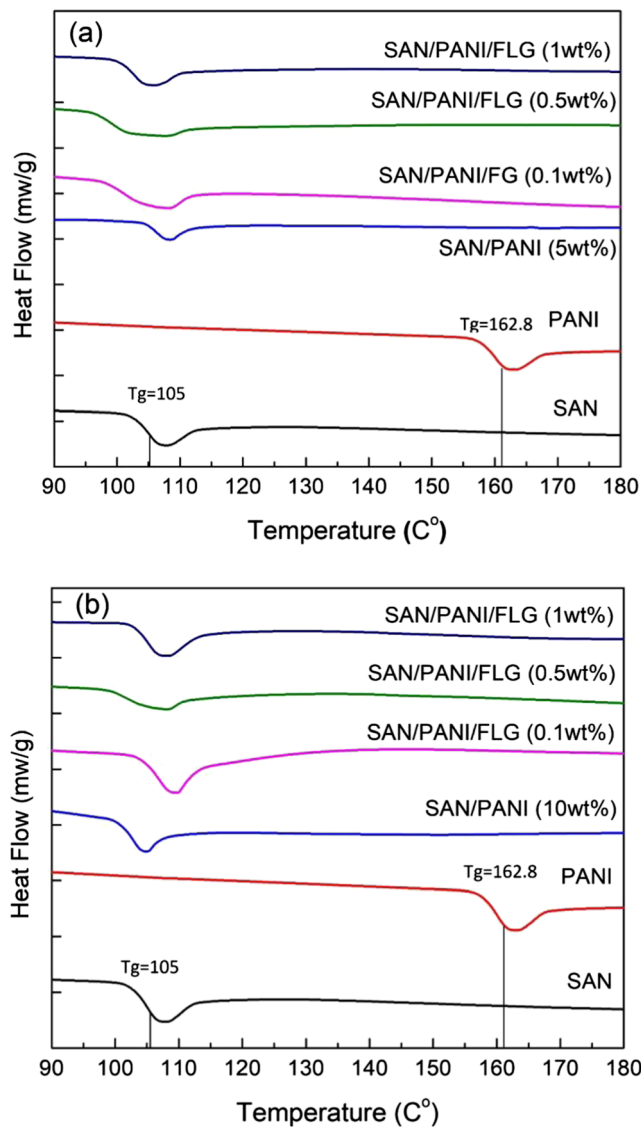


Fig. 2 Differential scanning calorimetry (DSC) results for (a) SAN, PANI, SAN/PANI-5.0/FLG hybrid composites, **b** SAN, PANI, SAN/PANI-10%/FLG hybrid composites

28.6 MPa, 1.03 GPa, respectively. Similar work has been reported by Zhang et al. [36] in which the mechanical behavior of Epoxy/GN hybrid polymer nanocomposites increased as the concentration of graphene oxide coated nano diamonds increased in Epoxy matrix. Maximum fluxirial strength of 155 MPa and maximum young’s modulus of 3.2 GPa were reported at 0.2 wt% concentration of GN. Similarly GO also enhanced the mechanical behavior at 0.2 wt% concentration but the increment is less than GN nano filler.

The stress-strain curve for hybrid composites SAN/PANI-10 with varying FLG loadings (Fig. 4) show similar mechanical behavior as shown by SAN/PANI-5.0 with FLG loading. At 10 wt% loading of PANI in SAN matrix, the mechanical response was significantly affected, which reduced the strain at break from 4.9% to 2.1%, while the tensile strength and

Fig. 3 Stress strain graph of SAN/PANI-5.0/ FLG hybrid composites (a), Tensile strength (c), Modulus (d) of SAN/PANI-5.0/ FLG hybrid composites

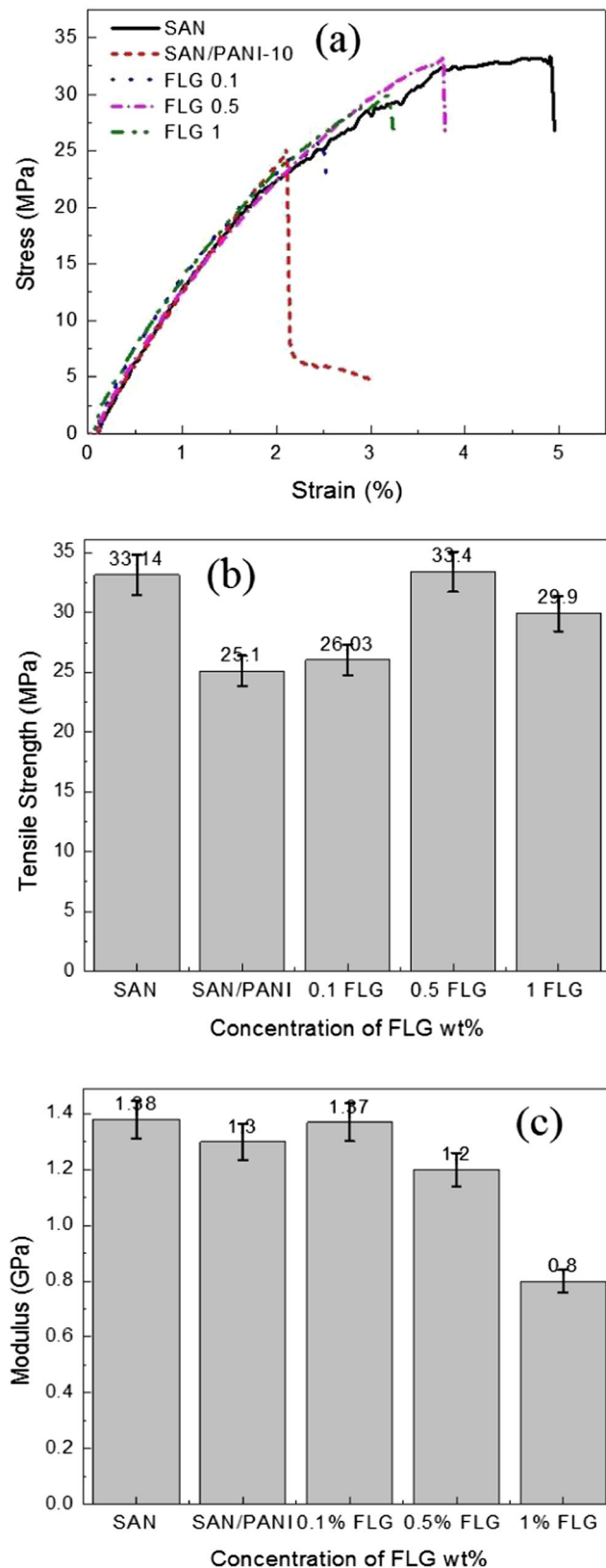


Fig. 4 Stress strain graph of SAN/PANI-10/ FLG hybrid composites (a), Tensile strength (b), Modulus (c) of SAN/PANI-10/FLG hybrid composites

modulus reduced from 33.14 MPa to 25.1 MPa and 1.38 GPa to 1.3 GPa, respectively. However, with addition of FLG (0.1 wt% & 0.5 wt%), both Young's modulus and tensile strength attains the base polymer values (1.37 GPa & 33.4 MPa). Further increase in FLG concentration to 1 wt% reduces the tensile strength and modulus to 29.9 MPa and 0.8 GPa, respectively.

Overall good mechanical response is shown in both the hybrid composites samples with varying concentration of FLG, as tensile strength and modulus both shows an increasing trend probably due to the constraining effect of FLG [37], but surprisingly a toughening effect is also observed in the system. The toughness increase may be attributed to the alignment of SAN/PANI polymer blends chains between the spaces of FLG, which consequently reduces the entanglement density and results in the increase of localized free volume. Hence the polymer chains mobility increases, which results in an increased toughness [38]. Possibly, FLG is not only physically associated well with the polymer chains but also dispersed uniformly in the system. The physical association of FLG might occur due to the interaction among oxygen containing groups present in FLG [31] with the polymer chains. Secondary bonding between FLG and polymer chains produces a good interface which helps in transferring the stress from polymer to FLG, thus increasing both tensile strength and modulus. The reduction in mechanical response with PANI incorporation is possibly due the formation of heterogeneous morphology of PANI phase in SAN matrix, which effects the packing arrangement of polymer chains, thereby reducing the tensile strength of SAN/PANI blends. Similar response of PANI has also been reported by B. G. Soares et al. [39], who worked on styrene-butadiene-styrene (SBS)/PANI system in which the tensile strength of SBS was reduced from 21 to 1.0 MPa by the addition of 30 wt% PANI.

To analyze the impact of PANI and FLG on the hardness of SAN polymer, micro hardness test is performed as shown in Fig. 5. Same trend is noticed for the increment in hardness values as it was evident in the tensile properties of SAN/PANI/FLG hybrid composites, showing significant increase in hardness with the addition of FLG in SAN/PANI polymer blend. In SAN/PANI-5/FLG hybrid composites the inclusion of PANI at 5 wt% reduces the hardness value from 26.2 to 23.8 HV. However a gradual increase in hardness is observed with the addition of FLG in SAN/PANI-5 polymer blend, with maximum increase of 273.5% in hardness from 23.8 to 88.9 HV at 0.5 wt% concentration of FLG. Further addition of FLG to 1 wt% slightly reduces the hardness value from 88.9 to 85.7 HV. Likewise in SAN/PANI-10/FLG hybrid composites the addition of PANI first reduces the hardness values, and then increases with the addition of FLG. Maximum increase of 237.4% i.e. from 19.5 to 65.8 HV is noticed at 0.5 wt% concentration of FLG in SAN/PANI-10 polymer

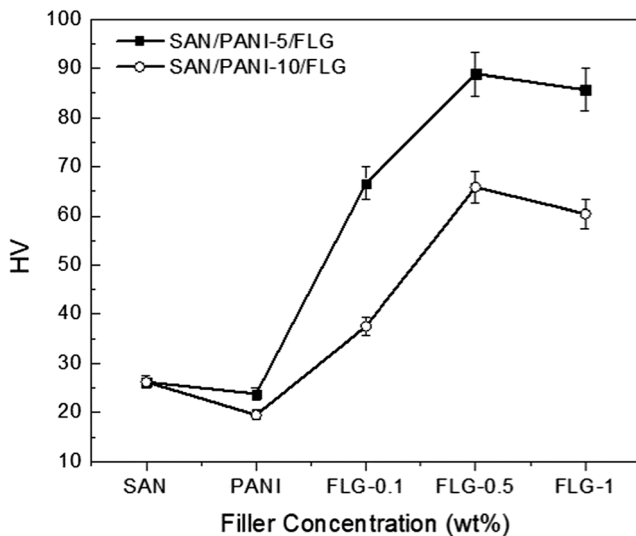


Fig. 5 Micro Vicker hardness (HV) graph of SAN/PANI-5/FLG and SAN/PANI-10/FLG hybrid composites at different FLG concentrations

blend. Recently Kaiser et al. [13] reported an increase of 1370% i.e. from 9.3 to 128 HV in hardness of ABS with the incorporation of FLG at 1.2 vol%. Such prominent increase in hardness of SAN/PANI polymer blend with the addition of FLG in both cases (SAN/PANI-5/FLG, SAN/PANI-10/FLG) can be attributed to the 2-D structure of FLG, as 2-D platelet of graphene causes more effective deformation of SAN/PANI polymer blend, thus performing a uniform dispersion resulting in significant increase in hardness.

Dielectric properties

Figures 6 and 7 shows the behavior of dielectric constant (ϵ') and dielectric loss (ϵ'') of SAN/PANI-5.0 and SAN/PANI-10 polymer blends with varying concentration of FLG. Both parameters were measured using impedance analyzer as a function of changing frequency at ambient temperature, respectively. SAN is a non-conductive polymer and with no dipoles, resulting in zero polarization and thus its dielectric properties are independent of alternating frequency. The incorporation of PANI and FLG in SAN polymer is responsible for the increment in ϵ' and ϵ'' of SAN in the lower frequency range, while at higher frequencies the value of ϵ' and ϵ'' tends to reduce and are close to each other for all concentrations of FLG. In SAN/PANI-5.0 polymer blend system the ϵ' , ϵ'' continuously increases with increasing concentration of FLG's in lower frequency range (Fig. 6a, b). The maximum increment in ϵ' and ϵ'' is noticed at 1 wt% concentration of FLG in SAN/PANI-5 wt% i.e. from 1.9 to 2.3, which is 18% increase in ϵ' and 0.02 to 5.48, which is a 22% increase in ϵ'' at 100 Hz frequency. Figure 7a, b shows the behavior of ϵ' and ϵ'' for SAN/PANI-10 wt% blend as a function of frequency with varying amounts of FLG. At 0.1 wt% of FLG in SAN/PANI-10 wt%, a maximum increase is observed for both ϵ' and ϵ'' , from 1.9 to

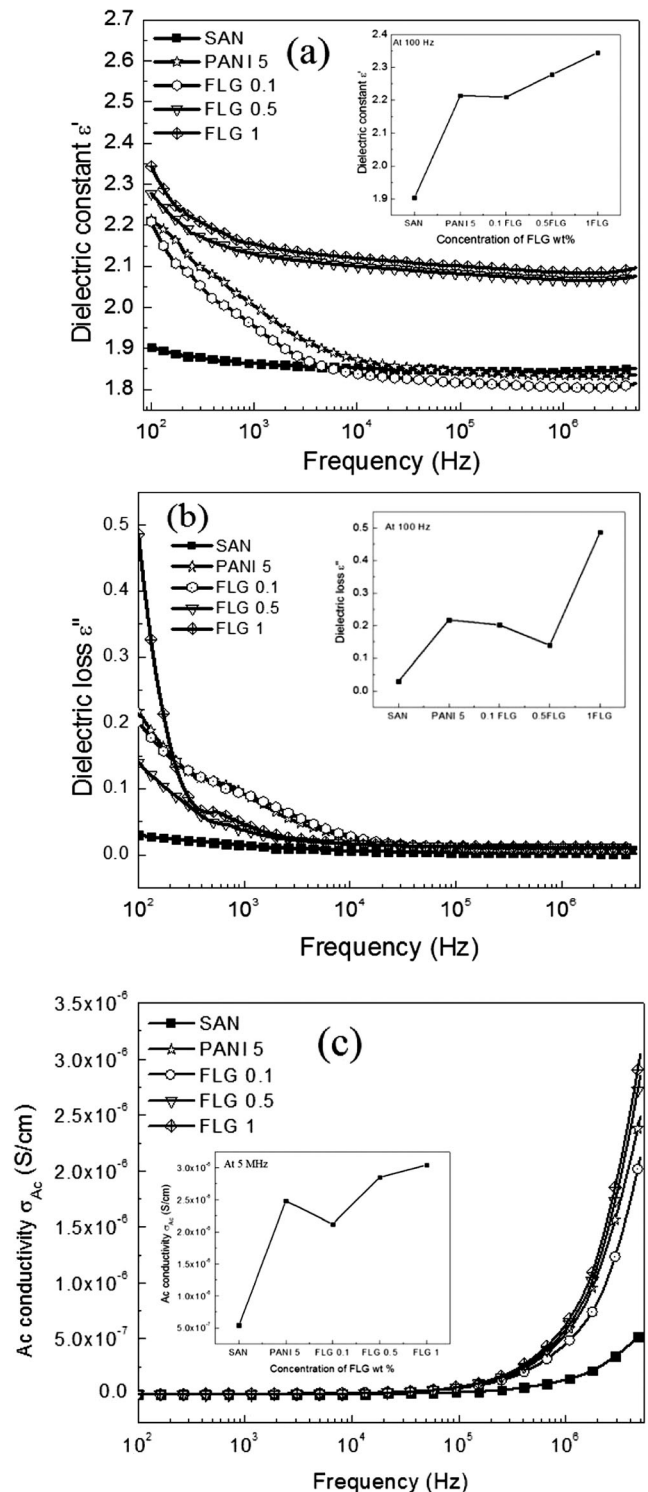


Fig. 6 Dielectric constant (a), Dielectric loss (b), and Ac conductivity (c) of SAN/PANI-5.0/FLG hybrid composites. The inset shows the values of Dielectric constant and Dielectric loss at 100 Hz, and Ac conductivity at 5 MHz with varying concentration of FLG

39.2 and 0.02 to 979.06, which is an increase of 95% and 99%, respectively. Furthermore, the increase in FLG concentration up to 1.0 wt%, ϵ' and ϵ'' values are decreased to 3.69 and 0.71, respectively. Recently, similar results were reported

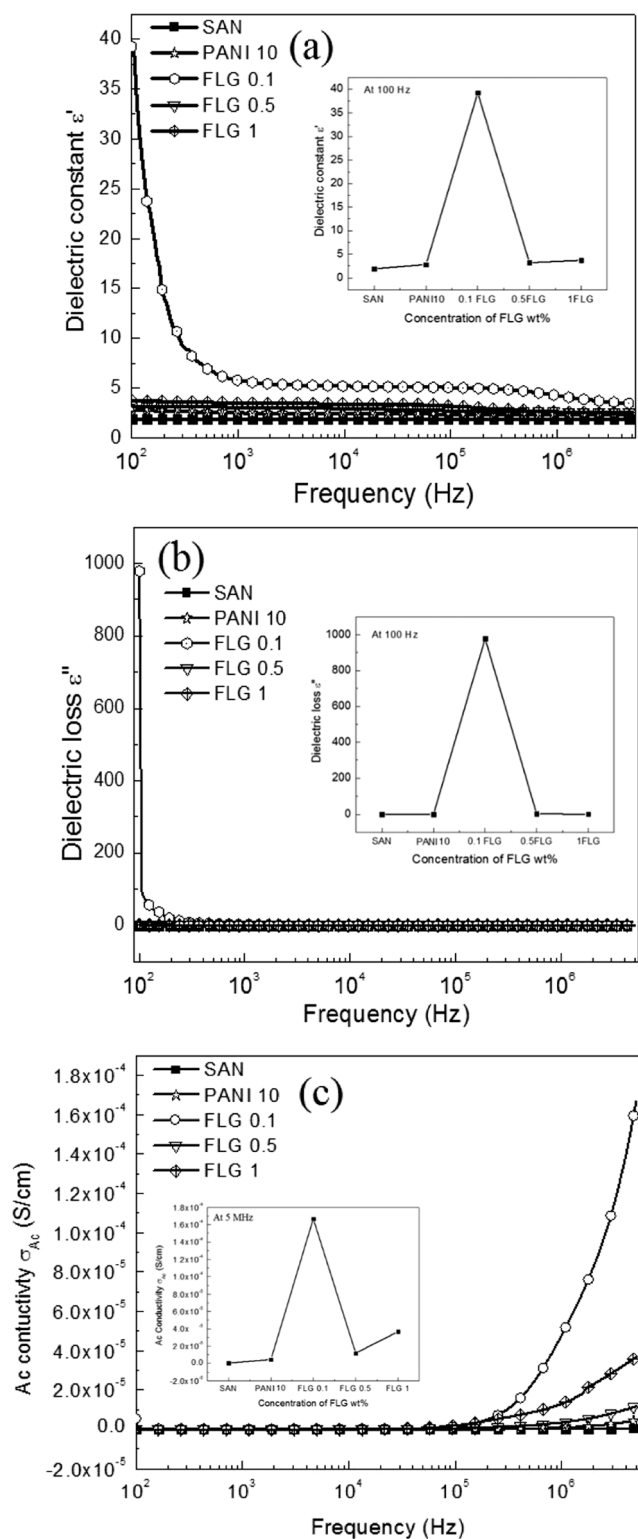


Fig. 7 Dielectric constant (a), Dielectric loss (b), and Ac conductivity (c) of SAN/PANI-10/FLG hybrid composites. The inset shows the values of Dielectric constant and Dielectric loss at 100 Hz, and Ac conductivity at 5 MHz with varying concentration of FLG

by Choudhary. [40] that the dielectric constant at 100 Hz of PEO-PMMA polymer blend increased from 3 to 9 with the

increasing concentration of PEO from 25 wt% to 75 wt% in PMMA matrix at 0 wt% concentration of SiO₂. Moreover, at 3 wt% concentration of SiO₂ in PEO-PMMA polymer nanocomposites the increasing concentration of PEO increased the dielectric constant from 3.5 to 8 at 100 Hz frequency. Similarly, Deshmukh et al. [41] examined the dielectric behavior of PVA/PEG polymer blend and PVA/PEG/GO hybrid polymer composites, and found out that by adding GO to PVA/PEG polymer blend at 3 wt% concentration the dielectric constant increased to 664.39 (50 Hz, 150 °C), which is 60% greater than the dielectric constant of PVA and 20% greater than the dielectric constant of PVA/PEG.

The increase in dielectric behavior (ϵ' , ϵ'') in both the systems at lower frequencies is due to Maxwell-Wagner polarization originating from the accumulation of space charges at the insulator-conductor interfaces or electric dipoles. Dipoles or space charges get enough time for their orientation to the applied electric field at lower frequencies, resulting in high polarization. Polarization effect does not appear at elevated frequencies because the change in electric field is rapid for the space charges and electric dipoles to respond to the applied alternating frequency. Percolation concentration is noticed at 0.1 wt% concentration of FLG in SAN/PANI-10 polymer at which both ϵ' , and ϵ'' shows maximum increase, as further increase in the concentration reduces dielectric property, which is discussed by number of researchers [42, 43].

AC conductivity σ_{AC} of pure SAN and SAN/PANI-5 & 10 with FLG, hybrid composites has been shown in Figs. 6c and 7c. The AC conductivity of samples were studied at ambient temperature with respect to alternating frequency with varying concentration of FLG's. In both hybrid composite systems the σ_{AC} increases with the increase in frequency as well as with the increase in concentration of FLG's. Maximum increase ($3.04E-6$ S/cm) in σ_{AC} is observed for SAN/PANI-5.0/FLG hybrid composite at 1 wt% loading of FLG's in Fig. 5c. The same behavior of σ_{AC} was observed for SAN/PANI-10 system with FLG's with one exception that percolation threshold concentration of 0.1 wt% of FLG's was noticed in higher frequency region, with increase in σ_{AC} up to $1.66E-4$ S/cm Fig. 6c. Gu, et al. [44] recently reported that AC conductivity of fGNPs/FREP increased from 1×10^{-5} S/cm to 5×10^{-4} S/cm at the 30 wt% concentration of fGNPs in FREP polymer matrix, which corresponds to formation of conductive network inside FREP. Reduction in σ_{AC} is observed when the concentration of FLG exceeds 0.1 wt%. The formation of conductive pathways above the percolation concentration may be responsible for the decrease in σ_{AC} . The increase in σ_{AC} at higher frequency is probably due to the hopping mechanism i.e. at higher field strength the dipoles are reshaped such that they overlap each other and the electrons start to jump from one dipole to another. To compare, all the values of ϵ' , ϵ'' at 100 Hz and σ_{AC} at 5 MHz for SAN, SAN/PANI polymer blends and SAN/PANI/FLG hybrid composites are listed in Table 1.

Table 1 The values of ϵ' , ϵ'' , and SE_T at 100 Hz, σ_{AC} at 5 MHz for SAN, SAN/PANI polymer blends and SAN/PANI/FLG hybrid composites

Samples	100 (Hz)		5 (MHz)
	ϵ'	ϵ''	σ_{AC} (S/cm)
SAN	1.903	0.029	5.38E-07
SAN/PANI (5 wt%)	2.214	0.218	2.48E-06
FLG (0.1 wt%)	2.209	0.202	2.11E-06
FLG (0.5 wt%)	2.278	0.140	2.85E-06
FLG (1 wt%)	2.344	0.487	3.04E-06
SAN/PANI (10 wt%)	2.794	0.258	4.50E-06
FLG (0.1 wt%)	39.249	979.060	1.66E-04
FLG (0.5 wt%)	3.195	2.549	1.17E-05
FLG (1 wt%)	3.698	0.711	3.67E-05

EMI shielding

EMI shielding is the capability of material to interact with the incoming EM wave and reduces its effect by absorbing or reflecting the EM waves. Total EMI shielding SE_T of a specimen is calculated by their reflection (SE_R), absorption (SE_A) shielding efficiencies, and multiple interaction (SE_I) of EM waves inside the shielding material. SE_T can be represented by the following Eq. (4).

$$SE_T = SE_A + SE_R + SE_I = 10 \log \frac{I_{IN}}{I_{out}} \tag{4}$$

Where I_{IN} and I_{out} represents the incident and transmitted electromagnetic waves through a shielding specimen, respectively. The unit of measurement for shielding efficiency is indicated by decibel (dB). The third term SE_I (internal reflection) in Eq. (4) is a positive or negative correction term, which is usually neglected when the $SE_R > 10$ dB. Reflection shielding efficiency (SE_R) is related to the interaction of EM waves with moving charges (holes or electron), which results in reflection loss. On the other hand the SE_A is due to the existence of magnetic or electric dipoles in the shielding specimen, causing the EM waves to be absorbed and then emitted in the form of heat by the shielding material. The transmitted EM waves are maximally attenuated by a shielding material either by reflection or absorption for better EMI shielding. To determine the total EMI shielding for both SAN/PANI/FLG hybrid composites following equations are used (5, 6, 7).

$$SE_A = 8.8\alpha l \tag{5}$$

$$SE_R = 20 \log \frac{|1+n|^2}{4|n|} \tag{6}$$

$$SE_I = 20 \log \left| 1 - \frac{\exp(-2\gamma l)^2}{(1+n)^2} \right| \tag{7}$$

The thickness of the sample is represented by l , whereas α , n and γ parameters are calculated by the following expression.

$$\alpha = \frac{2\pi}{\lambda} \sqrt{\frac{\epsilon'}{2} (\sqrt{1 + \tan^2 \delta})} \tag{8}$$

$$n = \sqrt{\frac{\epsilon' (\sqrt{1 + \tan^2 \delta} \pm 1)}{2}} + i \sqrt{\frac{\epsilon' (\sqrt{1 + \tan^2 \delta} \pm 1)}{2}} \tag{9}$$

$$\gamma = \left(\frac{2\pi}{\lambda}\right) \sqrt{\frac{\epsilon' (\sqrt{1 + \tan^2 \delta} \pm 1)}{2}} + i \left(\frac{2\pi}{\lambda}\right) \sqrt{\frac{\epsilon' (\sqrt{1 + \tan^2 \delta} \pm 1)}{2}} \tag{10}$$

The terms, λ , ϵ' and $\tan \delta$ in Eqs. 8–10 shows the wave length of incoming EM wave, dielectric constant and dissipation factor of the shielding specimen, respectively. The \pm sign is added to the above equations in order to balance the positive and negative values of dielectric constant.

SE_A , SE_R , and SE_I are calculated for both hybrid composites using Eqs. (5, 6, 7) and then plotting them against varying frequency is shown in (Figs. 8 and 9). Absorption shielding efficiency (SE_A) for both systems shows no increase in lower frequency range, but as the frequency is increased to higher values the SE_A increases (Figs. 8a and 9a). An increasing trend is observed for the reflection shielding efficiency (SE_R) in the lower frequency range for both hybrid composites, but as the frequency is increased the SE_R reduces to lower values (Figs. 8b and 9b). Total EMI shielding (SE_T) follows the same trend as that of reflection loss in both hybrid systems with varying concentration of FLG, because there is no noticeable increase in SE_A (Figs. 8c and 9c).

Maximum total shielding effectiveness of 1.2 dB was noticed at 100 Hz for SAN/PANI-5.0 with FLG. The addition of FLG in SAN/PANI-5.0 polymer blend do not improve the shielding effectiveness of hybrid composite, probably the incorporation of FLG disrupts the conductive network formation, moreover there is no significant increase in dielectric constant and dielectric loss by the addition of FLG in SAN/PANI-5.0 polymer blend, which results in no increase of shielding effectiveness Fig. 8c. The highest value of total shielding effectiveness (SE_T) of 24.3 dB at 100 Hz frequency is observed at 0.1 wt% loading of FLG in SAN/PANI-10

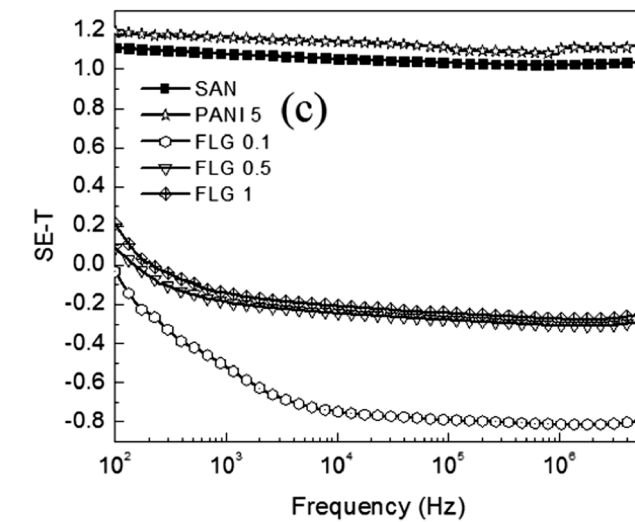
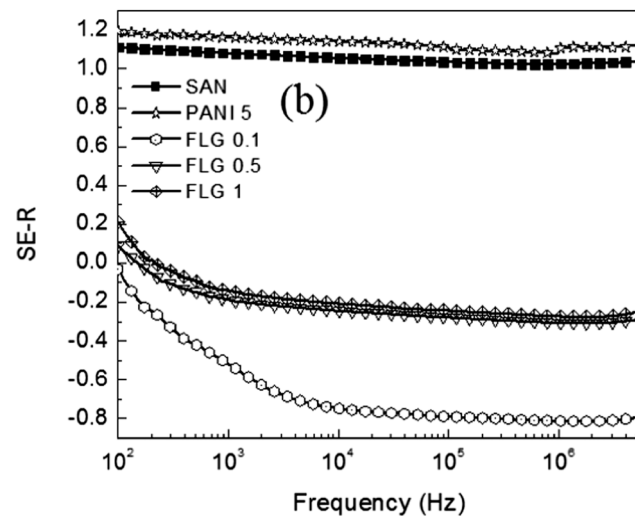
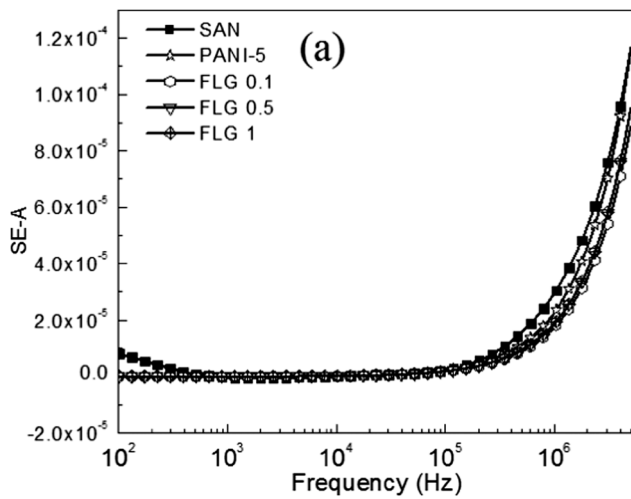


Fig. 8 SE_A , Absorption shielding efficiency (a), SE_R , Reflection shielding efficiency (b), SE_T , Total shielding efficiency (c) of SAN/PANI-5.0/FLG hybrid composites

polymer blend, owing to the percolation concentration having maximum values of dielectric constant and dielectric loss

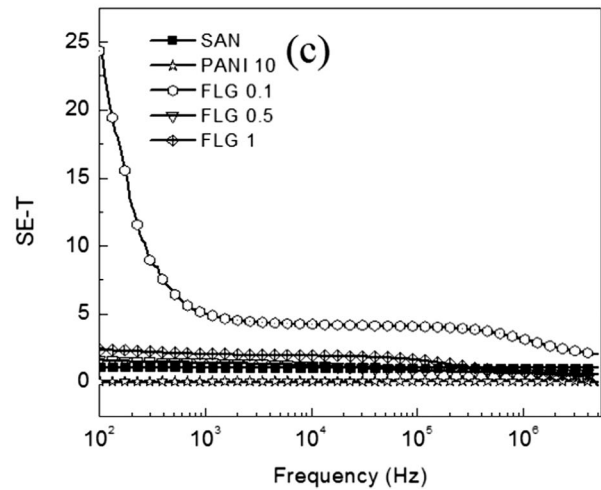
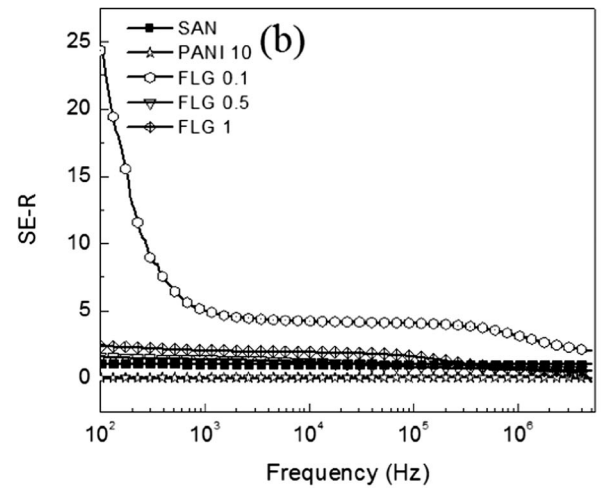
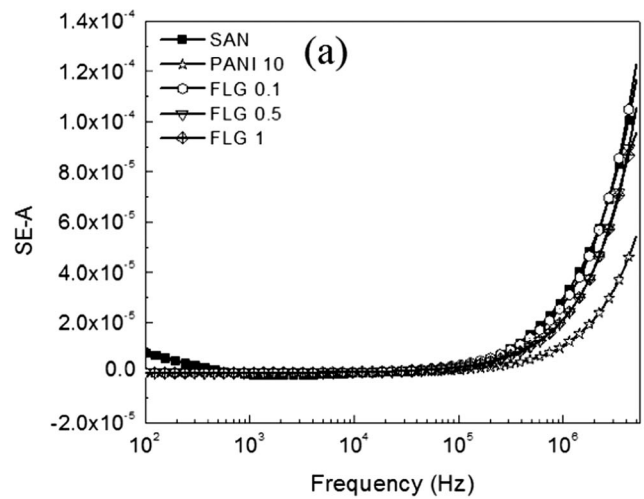


Fig. 9 SE_A , Absorption shielding efficiency (a), SE_R , Reflection shielding efficiency (b), SE_T , Total shielding efficiency (c) of SAN/PANI-10/FLG hybrid composites

(Fig. 9c). The tendency of SE_T validates the interconnected network formation of PANI and FLG in SAN polymer matrix at 0.1 wt% loading of FLG. The conductive network

formation enables the shielding material to maximally attenuate the EM waves by increasing the reflection loss. Recently Khan et al. [45] studied the total shielding efficiency (SE_T theoretical) for PVA/PANI/FLG hybrid composites prepared by solution casting technique in the frequency range of 100 Hz to 5 MHz. The maximum SE_T of 99 dB was observed at 0.1 wt% concentration of FLG in PVA/PANI-10 wt% polymer blend at 100 Hz, whereas the thickness of sample remained at ~ 0.1 mm. Similar results were reported earlier by Panwar et al. [46] that SE_T (theoretical) of 201 dB was observed at a frequency of 1.57 GHz for SAN-GS polymer nano composite at a concentration of 20 wt% of GS (graphene sheets) in SAN matrix.

The sample thickness plays a main role in increasing the shielding efficiency. The effect of thickness was reported by Mauro et al. [47] in the shielding efficiency of hybrid material of polyaniline/organoclay nanocomposites and EPDM rubber. Highest shielding efficiency of -11 dB was noticed at a frequency 11 to 12 GHz at 30 wt% concentration of PANI/organoclay, which shifted to -10 dB at a frequency of 9 to 10 GHz, as the thickness of the sample changed from 1.5 mm to 3 mm respectively. The samples were tested from 8 to 12 GHz frequency and shielding efficiency shifted from higher frequency to lower frequency. Similar results were reported by Joshi et al. [48] for the shielding efficiency of epoxy/PANI-graphene nano ribbons hybrid composite, in which the shielding efficiency increased from -44 dB to -68 dB as the thickness of sample increased from 1.7 mm to 3.4 mm at 5 wt% concentration of graphene nano ribbons in epoxy/PANI system. Promising results are shown by SAN/PANI/FLG hybrid composite system at a thickness ~ 0.15 mm, which is much less than the reported thickness of the sample.

Conclusion

The research work carried out on SAN/PANI/FLG hybrid polymer composites showed improvement in dielectric, EMI shielding, and mechanical characteristics. Only two concentrations of PANI i.e. at 5 wt% and 10 wt% were used in SAN matrix to prepare SAN/PANI polymer blends, in which FLG were dispersed at 0.1 wt%, 0.5 wt% and 1 wt% concentrations. In SAN/PANI-5.0 polymer blend the incorporation of FLG significantly enhances the mechanical properties i.e. the tensile strength increases by 60.2% and young modulus increases by 13.6%, whereas the dielectric and EMI shielding properties were slightly effected. However, a 95% increase in the dielectric and EMI shielding response (24.3 dB) was seen at 0.1 wt% loading of FLG in SAN/PANI-10 polymer blends, respectively. The increase in mentioned properties can be attributed to the network formation of both PANI and FLG in SAN matrix. In comparison to SAN/PANI

polymer blends, the promising mechanical and dielectric results of SAN/PANI/FLG hybrid composite system make them suitable candidate for microwave absorption applications.

Acknowledgements We thank Mr. Tanveer Zia for sample support and his valuable input.

Author's contribution ANK and RJ supervised and designed the experiments and co-wrote the manuscript. SS and MK helped in simulation model for plotting EMI shielding behavior and co-wrote the manuscript. All the co-authors read and approved the final manuscript.

Funding The project was supported by the research grants from Higher Education Commission (HEC), Pakistan under the NRPUR&D Project-20-3052.

Data availability The information regarding datasets generated during and/or analyzed during the current study are available from the corresponding co-authors on reasonable request.

Compliance with ethical standards

Competing interest The authors declare that they have no competing interests.

Abbreviations SAN, Styrene Acrylonitrile; PAN, Polyaniline; FLG, Few Layer Graphene; EMI, Electromagnetic Interference; PVA, Polyvinyl Alcohol; GNS, Graphene Nano Sheets; AC, Alternating Current; rGO, Reduced Graphene Oxide; PS, Polystyrene; SDS, Sodium Dodecyl Sulphate; ANI, Aniline; APS, Ammonium Peroxide Sulphate

References

1. Wu Y, Wang Z, Liu X, Shen X, Zheng Q, Xue Q, Kim JK (2017) Ultralight graphene foam/conductive polymer composites for exceptional electromagnetic interference shielding. *ACS Appl Mater Interfaces* 9(10):9059–9069
2. Ting T-H, Wu K-H (2013) Synthesis and electromagnetic wave-absorbing properties of BaTiO₃/polyaniline structured composites in 2–40 GHz. *J Polym Res* 20(5):127
3. Pawar SP, Biswas S, Kar GP, Bose S (2016) High frequency millimetre wave absorbers derived from polymeric nanocomposites. *Polymer* 84:398–419
4. Liu F, Li Q, Cui J, Li Z, Yang G, Liu Y, Dong L, Xiong C, Wang H, Wang Q (2017) High-energy-density dielectric polymer nanocomposites with Trilayered architecture. *Adv Funct Mater* 27(20):1606292
5. Han M, Yin X, Wu H, Hou Z, Song C, Li X, Zhang L, Cheng L (2016) Ti₃C₂ MXenes with modified surface for high-performance electromagnetic absorption and shielding in the X-band. *ACS Appl Mater Interfaces* 8(32):21011–21019
6. Naidu KCB, Madhuri W (2017) Microwave processed bulk and nano NiMg ferrites: a comparative study on X-band electromagnetic interference shielding properties. *Mater Chem Phys* 187:164–176
7. Biswas S, Arief I, Panja SS, Bose S (2017) Absorption-dominated electromagnetic wave suppressor derived from ferrite-doped cross-linked graphene framework and conducting carbon. *ACS Appl Mater Interfaces* 9(3):3030–3039

8. Shahzad F, Alhabeab M, Hatter CB, Anasori B, Man Hong S, Koo CM, Gogotsi Y (2016) Electromagnetic interference shielding with 2D transition metal carbides (MXenes). *Science* 353(6304): 1137–1140
9. Shahzad F, Kumar P, Kim YH, Hong SM, Koo CM (2016) Biomass-derived thermally annealed interconnected sulfur-doped graphene as a shield against electromagnetic interference. *ACS Appl Mater Interfaces* 8(14):9361–9369
10. Ran J, Shen L, Zhong L, Fu H (2017) Synthesis of silanized MoS₂/reduced graphene oxide for strong radar wave absorption. *Ind Eng Chem Res* 56(38):10667–10677
11. Wang Y, Chen D, Yin X, Xu P, Wu F, He M (2015) Hybrid of MoS₂ and reduced graphene oxide: a lightweight and broadband electromagnetic wave absorber. *ACS Appl Mater Interfaces* 7(47):26226–26234
12. Idris FM, Hashim M, Abbas Z, Ismail I, Nazlan R, Ibrahim IR (2016) Recent developments of smart electromagnetic absorbers based polymer-composites at gigahertz frequencies. *J Magn Magn Mater* 405:197–208
13. Waheed Q, Khan AN, Jan R (2016) Investigating the reinforcement effect of few layer graphene and multi-walled carbon nanotubes in acrylonitrile-butadiene-styrene. *Polymer* 97:496–503
14. Ma J, Wang X, Cao W, Han C, Yang H, Yuan J, Cao M (2018) A facile fabrication and highly tunable microwave absorption of 3D flower-like Co₃O₄-rGO hybrid-architectures. *Chem Eng J* 339: 487–498
15. Song C, Yin X, Han M, Li X, Hou Z, Zhang L, Cheng L (2017) Three-dimensional reduced graphene oxide foam modified with ZnO nanowires for enhanced microwave absorption properties. *Carbon* 116:50–58
16. Feng W, Wang Y, Chen J, Wang L, Guo L, Ouyang J, Jia D, Zhou Y (2016) Reduced graphene oxide decorated with in-situ growing ZnO nanocrystals: facile synthesis and enhanced microwave absorption properties. *Carbon* 108:52–60
17. Zhang Y, Wang X, Cao M (2018) Confinedly implanted NiFe₂O₄-rGO: cluster tailoring and highly tunable electromagnetic properties for selective-frequency microwave absorption. *Nano Res* 11(3): 1426–1436
18. Shamsi R, Koosha M, Mahyari M (2016) Improving the mechanical, thermal and electrical properties of polyurethane-graphene oxide nanocomposites synthesized by in-situ polymerization of ester-based polyol with hexamethylene diisocyanate. *J Polym Res* 23(12):262
19. Bhawal P et al (2018) Fabrication of light weight mechanically robust short carbon fiber/ethylene methyl acrylate polymeric nanocomposite for effective electromagnetic interference shielding. *J Polym Sci Appl*:2017
20. Bhadra S, Khastgir D, Singha NK, Lee JH (2009) Progress in preparation, processing and applications of polyaniline. *Prog Polym Sci* 34(8):783–810
21. Kumar P, Shahzad F, Yu S, Hong SM, Kim YH, Koo CM (2015) Large-area reduced graphene oxide thin film with excellent thermal conductivity and electromagnetic interference shielding effectiveness. *Carbon* 94:494–500
22. Zhu D, Guo Q, Zheng Z, Matsuo M (2014) Thermal and dielectric investigations on the blends of κ-carrageenan and nano-structured polyaniline. *Synth Met* 187:165–171
23. Rose A, Guru Prasad K, Sakthivel T, Gunasekaran V, Maiyalagan T, Vijayakumar T (2018) Electrochemical analysis of graphene oxide/polyaniline/polyvinyl alcohol composite nanofibers for supercapacitor applications. *Appl Surf Sci* 449:551–557
24. Chaudhary A, Kumar R, Teotia S, Dhawan SK, Dhakate SR, Kumari S (2017) Integration of MCMBs/MWCNTs with Fe₃O₄ in a flexible and light weight composite paper for promising EMI shielding applications. *J Mater Chem C* 5(2):322–332
25. Arenas M et al (2014) Electrical and morphological properties of polyaniline–polyvinyl alcohol in situ nanocomposites. *Compos Part B* 56:857–861
26. Saboor A et al (2016) Effect of polyaniline on the dielectric and EMI shielding behaviors of styrene acrylonitrile. *J Mater Sci Mater Electron* 27(9):9634–9641
27. Panwar V, Mehra R (2008) Study of electrical and dielectric properties of styrene-acrylonitrile/graphite sheets composites. *Eur Polym J* 44(7):2367–2375
28. Jlassi K, Chandran S, Poothanari MA, Benna-Zayani M, Thomas S, Chehimi MM (2016) Clay/polyaniline hybrid through diazonium chemistry: conductive nanofiller with unusual effects on interfacial properties of epoxy nanocomposites. *Langmuir* 32(14):3514–3524
29. Shahzad F, Yu S, Kumar P, Lee JW, Kim YH, Hong SM, Koo CM (2015) Sulfur doped graphene/polystyrene nanocomposites for electromagnetic interference shielding. *Compos Struct* 133:1267–1275
30. Liang J, Wang Y, Huang Y, Ma Y, Liu Z, Cai J, Zhang C, Gao H, Chen Y (2009) Electromagnetic interference shielding of graphene/epoxy composites. *Carbon* 47(3):922–925
31. Janowska I, Vigneron F, Bégin D, Ersen O, Bernhardt P, Romero T, Ledoux MJ, Pham-Huu C (2012) Mechanical thinning to make few-layer graphene from pencil lead. *Carbon* 50(8):3106–3110
32. Jan R, Habib A, Abbasi H, Amir S (2015) Dielectric spectroscopy of high aspect ratio graphene-polyurethane nanocomposites. *Electron Mater Lett* 11(2):225–231
33. Abutalib M (2018) Insights into the structural, optical, thermal, dielectric, and electrical properties of PMMA/PANI loaded with graphene oxide nanoparticles. *Phys B Condens Matter*
34. Qi Y et al (2008) Thermal stability and glass transition behavior of PANI/α-Al₂O₃ composites. *J Therm Anal Calorim* 94(2):553–557
35. Qi Y, Zhang J, Qiu S, Sun L, Xu F, Zhu M, Ouyang L, Sun D (2009) Thermal stability, decomposition and glass transition behavior of PANI/NiO composites. *J Therm Anal Calorim* 98(2):533–537
36. Zhang Y, Rhee KY, Park S-J (2017) Nanodiamond nanocluster-decorated graphene oxide/epoxy nanocomposites with enhanced mechanical behavior and thermal stability. *Compos Part B* 114: 111–120
37. Jan R, Habib A, Akram MA, Zia TUH, Khan AN (2016) Uniaxial drawing of graphene-PVA nanocomposites: improvement in mechanical characteristics via strain-induced exfoliation of graphene. *Nanoscale Res Lett* 11(1):377
38. Khan AN, Hong P-D, Chaung W-T (2013) Relaxation behavior of poly(trimethylene 2, 6-naphthalate) in nanoclay confinement. *J Polym Res* 20(10):280
39. Soares BG, Leyva ME (2007) Effect of blend preparation on electrical, dielectric, and dynamical-mechanical properties of conducting polymer blend: SBS triblock copolymer/polyaniline. *Macromol Mater Eng* 292(3):354–361
40. Choudhary S (2018) Effects of amorphous silica nanoparticles and polymer blend compositions on the structural, thermal and dielectric properties of PEO–PMMA blend based polymer nanocomposites. *J Polym Res* 25(5):116
41. Deshmukh K, Ahamed MB, Sadasivuni KK, Ponnamma D, Deshmukh RR, Pasha SKK, AIMaadeed MAA, Chidambaram K (2016) Graphene oxide reinforced polyvinyl alcohol/polyethylene glycol blend composites as high-performance dielectric material. *J Polym Res* 23(8):159
42. Al-Saleh MH, Sundararaj U (2008) An innovative method to reduce percolation threshold of carbon black filled immiscible polymer blends. *Compos A: Appl Sci Manuf* 39(2):284–293

43. Mao C, Zhu Y, Jiang W (2012) Design of electrical conductive composites: tuning the morphology to improve the electrical properties of graphene filled immiscible polymer blends. *ACS Appl Mater Interfaces* 4(10):5281–5286
44. Gu J, Liang C, Zhao X, Gan B, Qiu H, Guo Y, Yang X, Zhang Q, Wang DY (2017) Highly thermally conductive flame-retardant epoxy nanocomposites with reduced ignitability and excellent electrical conductivities. *Compos Sci Technol* 139:83–89
45. Khan M et al (2017) Investigating mechanical, dielectric, and electromagnetic interference shielding properties of polymer blends and three component hybrid composites based on polyvinyl alcohol, polyaniline, and few layer graphene. *Polym Compos*
46. Panwar V, Kang B, Park JO, Park S, Mehra RM (2009) Study of dielectric properties of styrene-acrylonitrile graphite sheets composites in low and high frequency region. *Eur Polym J* 45(6): 1777–1784
47. Soto-Oviedo MA, Araújo OA, Faez R, Rezende MC, de Paoli MA (2006) Antistatic coating and electromagnetic shielding properties of a hybrid material based on polyaniline/organoclay nanocomposite and EPDM rubber. *Synth Met* 156(18–20):1249–1255
48. Joshi A, Bajaj A, Singh R, Anand A, Alegaonkar PS, Datar S (2015) Processing of graphene nanoribbon based hybrid composite for electromagnetic shielding. *Compos Part B* 69:472–477